IL NUOVO CIMENTO **41 C** (2018) 187
DOI 10.1393/ncc/i2018-18187-3

Colloquia: IWM-EC 2018

LCP Fast Emission *vs.* Evaporation from ^{46}Ti*

M. Cicerchia(1)(2)(*), F. Gramegna(1), D. Fabris(3), T. Marchi(1), M. Cinausero(1), G. Mantovani(1)(2), A. Caciolli(2)(3), G. Collazuol(2)(3), D. Mengoni(2)(3), M. Degerlier(4), L. Morelli(5), M. Bruno(6), M. D'Agostino(6), C. Frosin(6), S. Barlini(7), S. Piantelli(7), M. Bini(7), G. Pasquali(7), P. Ottanelli(7), G. Casini(7), G. Pastore(7), A. Camaiani(7), S. Valdré(7), D. Gruyer(5), N. Gelli(7), A. Olmi(7), G. Poggi(7), I. Lombardo(8), D. Dell'Aquila(9), S. Leoni(10), N. Cieplicka-Orynczak(11), B. Fornal(11) and V. Kravchuk(12)

(1) *INFN, Legnaro National Laboratory - Legnaro (PD), Italy*
(2) *Padua University, Physics and Astronomy Department - Padua, Italy*
(3) *INFN, Padua Department - Padua, Italy*
(4) *Science and Art Faculty, Physics Department, Nevsehir Haci Bektas Veli Univ. - Nevsehir, Turkey*
(5) *Grand Accélérateur National d'Ions Lourds - 14076 Caen, France*
(6) *INFN, Bologna Department and University, Physics and Astronomy Department - Bologna, Italy*
(7) *INFN, Florence Department and University, Physics and Astronomy Department - Florence, Italy*
(8) *INFN, Catania Department - Catania, Italy*
(9) *MSU Department of Physics and Astonomy - East Lansing MI, USA*
(10) *INFN, Milan Department and University, Physics and Astronomy Department - Milan, Italy*
(11) *Institute of Nuclear Physics, Polish Academy of Sciences - Krakow, Poland*
(12) *National Research Center "Kurchatov Institute" - Moscow, Russia*

received 3 December 2018

Summary. — The study of pre-equilibrium (or fast) emitted particles is a useful tool to examine nuclear clustering; to study how possible cluster structures affect nuclear reactions, the NUCL-EX Collaboration (INFN, Italy) is carrying out an extensive research campaign on pre-equilibrium emission of light charged particles from hot nuclei. In this framework, the reactions ^{16}O + ^{30}Si, ^{18}O + ^{28}Si and ^{19}F + ^{27}Al at 7 MeV/u have been measured at the GARFIELD+RCo array in Legnaro National Laboratories. After a general introduction on the experimental campaign, this contribution will focus on the analysis results obtained so far; effects related to the entrance channel and to the colliding ions cluster nature are emphasized through differences between the theoretical predictions and the experimental data.

(*) E-mail: cicerchia@lnl.infn.it

Creative Commons Attribution 4.0 License (http://creativecommons.org/licenses/by/4.0)

1. – Introduction

In the last decade, the NUCLEX Collaboration (INFN, Italy), has been engaged in an extensive reaserch campaign on fast emission of light charged particles (LCP) in order to study how possible cluster structures affect nuclear reactions [1-4]. During the early stages of the reaction, non-equilibrium processes play an important role in the dynamics of heavy-ion collisions; in particular, they contribute to determine the features of the remaining hot thermalized sources. The fast emissions issued by these processes depend both on the entrance channel mass asymmetry and on the beam velocity [5].

In this context, a comparative study of three systems has been conceived. The idea is to study them in two energy regimes: firstly, at energies close to the onset of the pre-equilibrium process, to evaluate its properties in a quite well-known framework; then, to carry out a following experiment of the same systems at higher bombarding energies, where the pre-equilibrium part is well assessed and may play a major role.

In this report, the first measurement is presented; four reactions are studied: ^{16}O+^{30}Si, ^{18}O+^{28}Si and ^{19}F+^{27}Al at 7 MeV/u and ^{16}O+^{30}Si at 8 MeV/u.

2. – The experiment

The experiment was performed at the Legnaro National Laboratory (LNL), where the four beams have been provided by the TANDEM acceleration system and have been used respectively onto the different thin (100 μg/cm^2) targets: ^{30}Si, ^{28}Si and ^{27}Al. The employed energies are close to the lower thresholds for the pre-equilibrium emission process. The GARFIELD plus Ring Counter (RCo) detector fully equipped with digital electronics [6, 7] has been used to detect LCP, light fragments (LF) and evaporation residues (ER).

Through central collisions and when the complete fusion occurs, the four studied cases all lead to the same compound nucleus, the excited ^{46}Ti, even if with slightly different excitation energies. Small differences in their de-excitation chain are expected, except for the cases ^{16}O+^{30}Si at 8 MeV/u and ^{18}O+^{28}Si at 7 MeV/u, which were chosen to populate the compound nucleus at the same excitation energy. On the other hand, the choice of the same beam energy (7 MeV/u) for three of the four reactions should imply that the non-equilibrium processes are compatible, given the same projectile velocity [5]. The main characteristics of the four reactions are shown in table I.

The main goal of this experiment is to measure and compare different mass entrance channel reactions with the aim of estimating the pre-equilibrium components. This will be done by analyzing the competition between fast and statistical emissions; by evaluating exclusive observables through correlation analysis and by comparison with model predictions. Moreover, information about the influence of structure effects, like α-clustering, will be investigated for medium mass systems.

TABLE I. – *The main characteristics of the reactions.*

Entrance channel	$E_{beam,lab}$ (MeV)	η	CN	E^* (MeV)	$\frac{\eta}{E^*}$
^{16}O+^{30}Si	111	0.30	^{46}Ti	88.0	0,00346
^{16}O+^{30}Si	128	0.30	^{46}Ti	98.4	0,00309
^{18}O+^{28}Si	126	0.22	^{46}Ti	98.5	0,00221
^{19}F+^{27}Al	133	0.17	^{46}Ti	103.5	0,00168

3. – Event selection

Since an evident oxigen-contamination of the Si and of the Al targets has been observed, a very strict selection on experimental data was performed for the subsequent analysis. In order to define quantitatively the amount of contaminants, a dedicated measurement was performed on the targets with RBS technique [8, 9], at the LNL AN-2000 accelerator: a ratio of about 1:1 was measured for the oxigen with respect to both ^{30}Si and ^{28}Si targets, while a ratio of 1:2 was present in the ^{27}Al target. The contaminant reactions were also simulated using the GEMINI^{++} and the HIPSE+SIMON codes; such simulations are then compared with the experimental data and analyzed. The experimental high contamination of the target is not separable from the other inclusive data due to the superposition with the deep inelastic collisions products. Therefore, it is not possible to study these "contaminant" reactions. Fortunately, the reactions of interest are well separable from the "contaminant" reactions and from the other reaction mechanisms. To avoid contaminated data, the considered events are those for which the total detected charge is larger than the 70% and the longitudinal momentum is around the unit; to select such specific events a graphical contour has been applied on the plot of correlation between total charge and longitudinal momentum. This graphical cut was read by the analysis program and applied not only to the experimental data but also to the simulated ones. As a consequence of this first data selection, the amount of the experimental selected events is around the 10% of the total detected events.

A further selection was applied asking for the detection of the light charge particles (detected in the whole apparatus: GARFIELD+RCo) in coincidence with at least one evaporation residue (in forward angles: RCo); such events characterize the central collisions. The combined effects of the two cuts (on Z_{tot} *vs.* q_z/q_{beam} and on Z *vs.* E_{lab}) imposed on the experimental data are analyzed and cross-checked in comparison with the same cuts imposed on the AMD+GEMINI^{++} simulation. In order to select only the event produced by fusion-evaporation reactions, an additional constraint was imposed to the selection of residues: in a "good" event only one fragment with a charge heavier than 6 can exist; in this way, the fission events are excluded from the selection.

4. – Simulation codes

The selected experimental observables have been compared with the simulations, produced with different codes based on theoretical models, to obtain a theoretical feedback. In particular, the code GEMINI^{++} by R. Charity [10] was used to describe the statistical decay of the compound nuclei produced in the reactions. In addition, the dynamical codes AMD by A. Ono [11] and HIPSE by D. Lacroix [12] were used to simulate the dynamical part of the reactions. The AMD code is based on a stochastic equation of motion for the Gaussian wave packets representing the colliding nucleons. It describes the cluster structure of the interacting particles and takes into accounts the particle-particle correlations. The HIPSE code is based on the sudden approximation and can describe the nuclear collisions in the intermediate energy range. Both codes can describe the first evolution path of the reactions; after a time, t, the GEMINI^{++} code has been coupled to dynamical model as afterburner to simulate in a statistical environment how the produced primary excited fragments decay, so to simulate the entire secondary particle and fragment production.

For the GEMINI^{++} code, a specific choice of the level density has been considered, which take into account the angular momentum induced deformation of the ^{46}Ti* nucleus,

already observed by A. May and co-workers [13]. Moreover, in order to take into account the effects of a possible deformation induced by temperature, different values of the parameter w have been considered: this parameter permits to simulate the emission from nuclei with a convolution of barriers going from $r + \mathrm{d}r$ to $r - \mathrm{d}r$, where $\mathrm{d}r = w\sqrt{T}$. In our case, we began by using the default value of $w = 1.0$ fm, which corresponds to an axes ratio $b : a$ of $2 : 1$; afterwards, values of $w = 0.0\,\mathrm{fm}$, which corresponds to a unique barrier of a spherical nucleus, and $w = 1.1\,\mathrm{fm}$, which corresponds to a ratio of the nucleus axes of $b : a = 2.2 : 1$ have been considered.

5. – The data analysis

A detailed analysis of experimental data in comparison with GEMINI^{++}, HIPSE+GEMINI^{++} and AMD+GEMINI^{++} simulations has been done for selected observables for the four reactions. In this report, we focus on the analysis of the complete events, selected imposing a total detected charge corresponding to the total entrance channel charge ($Z_p + Z_T = 22$).

In fig. 1 the comparison of experimental and simulated angular distribution of protons (left panels) and α-particles (right panels) are presented for the four reactions: ^{16}O+^{30}Si at 111 MeV (panels *a.* and *b.*), ^{16}O+^{30}Si at 128 MeV (panels *c.* and *d.*) ^{18}O+^{28}Si at 126 MeV (panels *e.* and *f.*) and ^{19}F+^{27}Al at 133 MeV (panels *g.* and *h.*). The experimental data are represented as black dots, while the simulation as colored triangles: pink for the AMD + GEMINI^{++}, orange for the HIPSE + GEMINI^{++} and the three GEMINI^{++} are respectively green ($w = 0.0\,\mathrm{fm}$), red ($w = 1.0\,\mathrm{fm}$) and blue ($w = 1.1\,\mathrm{fm}$). The simulations are normalized to the relative number of residues: $\frac{\#_{res,exp}}{\#_{res,sim}}$. Starting from the proton angular distributions (left panels), all the simulations overpredict them in the $\theta_{lab} = 29.5°$–$150.4°$ angular range, corresponding to the GARFIELD angular range, while they are reasonably reproduced in the very forward region (RCo). The experimental underproduction of protons is more evident in the case of the ^{16}O+^{30}Si at 111 MeV, that is the reaction at lower excitation energy, and decrease increasing the excitation energy of the systems. On the contrary, the very forward angular region is well accounted for by all simulations in the cases of the two ^{16}O induced reactions (panels *a.* and *c.*), some differences appear in the ^{18}O+^{28}Si at 126 MeV case (panel *e.*) and finally all simulations overestimate the proton angular distributions (panel *g.*). For what concerns α-particles (right panels), the central angular region ($\theta_{lab} = 29.5°$–$81.5°$) is well accounted for by all the simulations; GEMINI^{++} with $w = 1.0\,\mathrm{fm}$ and HIPSE+GEMINI^{++} do not reproduce neither the forward nor the backward directions, while the other three simulations are better describing the total distribution apart from the very forward angular region, totally underestimated. The large underestimation of α-particles in forward region ($\theta_{lab} = 8.8°$–$17.4°$) decrease increasing the excitation energy.

For a faster comparison and a summary of the experimental findings the differences between the experimental and the simulated yields for the three angular region: backward, that is $\theta_{lab} = 97.5°$–$150.4°$, central, that is $\theta_{lab} = 29.5°$–$82.5°$, and forward that is $\theta_{lab} = 8.8°$–$17.4°$, are reported in the fig. 2, where the yields differences are displayed toward the $\frac{\eta}{E^*}$ parameter, where the ratio of the excitation energy and the entrance channel mass asymmetry parameters (the values of this parameter for the four reactions are listed in the last column of table I). The choice to use a composite parameter, instead of just η or E^* alone, derives from the fact that this combination of the two are something that differently characterize the four reactions and takes into account both effects of different

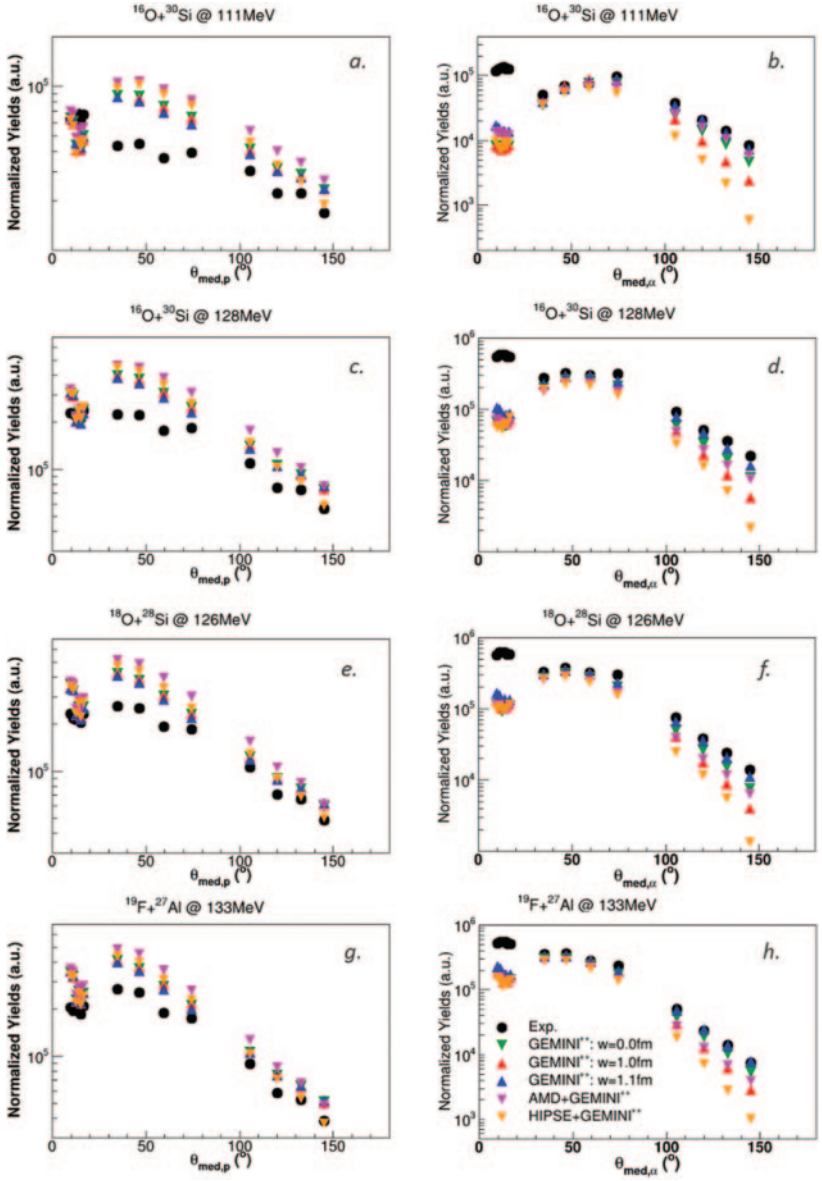

Fig. 1. – Comparison of experimental and simulated (GEMINI^{++} with $w = 0.0$ fm in green, with $w = 1.0$ fm in red, $w = 1.1$ fm in blue; AMD+GEMINI^{++} in pink; HIPSE+GEMINI^{++} in orange) proton and α angular distributions for the four reactions studied. See text for details.

temperature/decay path of the emitting nuclei and effects due to initial colliding partner mass asymmetries. To guide the eye a dashed line corresponding to 0 difference is also plotted in the figure. An opposite trend is observed for protons and α-particles, that is the more α-particles are underevaluated by codes the more protons are overevaluated. The best code seems to be in an overall picture the GEMINI^{++} with $w = 1.1$ fm. In the forward region a larger discrepancy is observed for α-particles: in fact, at all energies an

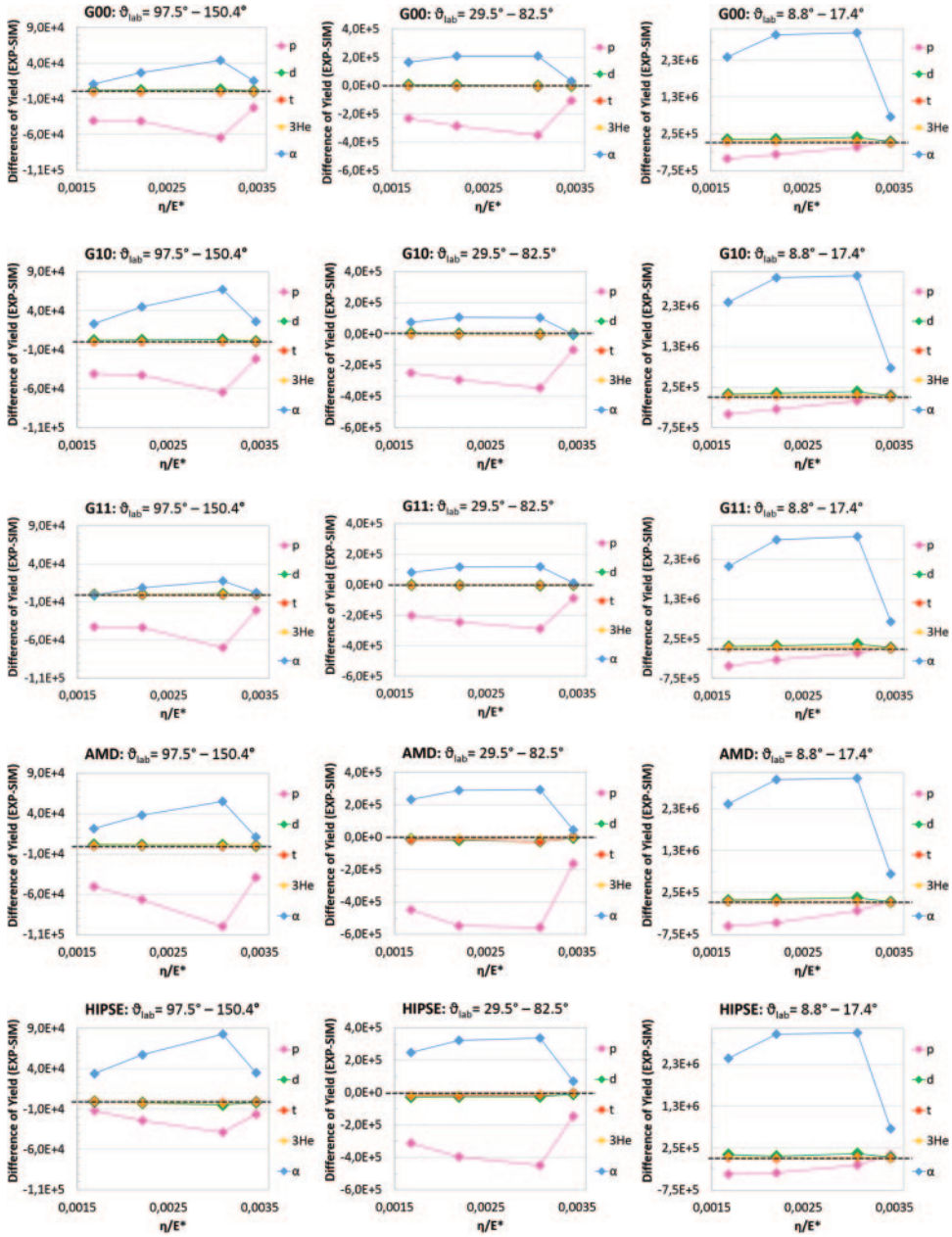

Fig. 2. – Differences between experimental data and simulations of the integrated angular yields as a function of η/E^*. G00, G10, G11, AMD, HIPSE means respectively GEMINI^{++} with $w = 0.0$ fm, with $w = 1.0$ fm and $w = 1.1$ fm, AMD+GEMINI^{++} and HIPSE + GEMINI^{++}. See text for more details.

oveproduction in the forward region was observed. On the contrary, protons are better represented, even still not completely.

The reaction with minor discrepancies, for what concerns the experimental angular distribution yields with respect to models, is the ^{16}O at 111 MeV one, that is the forth

value on the graphs in the figure, corresponding to $\frac{\eta}{E^*} = 0,0035$. The ^{16}O at 128 MeV and ^{18}O at 126 MeV reactions show similar trends except in the case of backward angles, where a larger discrepancy is observed for the ^{16}O case with respect to ^{18}O. The ^{19}F at 133 MeV reaction shows an intemediate situation demonstrating that these differences are not scaling only with the excitation energy.

6. – Conclusions and perspectives

In order to probe the competition between thermal and fast emission processes and the possible α-clustering effects on dynamics, the comparative study of the four reactions, ^{16}O+^{30}Si at 8 MeV/u, ^{16}O+^{30}Si, ^{18}O+^{28}Si and ^{19}F+^{27}Al at 7 MeV/u, has been carried out at LNL. In this paper, the attention has been focused on the complete events; differences between the experimental and the predicted observables put into evidence effects related to the entrance channels. In particular, the overproduction of α-particles of forward angles represents a signature of the onset of fast emission. To understand if the pre-equilibrium process is well accounted for by theory, a more quantitative analysis is needed. Indeed, the differences in specific multiplicity channels have been noticed with consequences on the branching ratios and Q-value distributions. Lastly, to complete this experimental campaign, new measurements of the same systems (^{16}O+^{30}Si, ^{18}O+^{28}Si and ^{19}F+^{27}Al) need to be carried out at higher energies (12–16 AMeV), where larger pre-equilibrium yields and higher excitation energies are foreseen: in fact, the analysis of correlations between LCP particles, especially in long α-decay chains ($M_\alpha \geq 3$) events, are necessary to constraint the dynamics and to draw conclusions on the differences among the studied systems and on their possible link to structural effects of the colliding partners. Further study on the same field will be done also using the new apparatus developed by our Collaborations ATS and OSCAR [14].

REFERENCES

[1] Morelli L. *et al.*, *J. Phys. G*, **41** (2014) 075107; 075108.
[2] Fabris D. *et al.*, *EPJ Web of Conferences*, **163** (2017) 00016.
[3] Kravchuk V. L. *et al.*, *EPJ Web of Conferences*, **2** (2010) 10006.
[4] Fotina O. V. *et al.*, *Int. J. Mod. Phys. E*, **19** (2010) 1134.
[5] Hogson P. E. and Běták, *Phys. Rep.*, **374** (2003) 1.
[6] Gramegna F. *et al.*, *IEEE Nucl. Sci. Symp. Conf. Proc.*, **2** (2004) 1132.
[7] Bruno M. *et al.*, *Eur. Phys. J. A*, **49** (2013) 128.
[8] Chu W. K., Mayer J. M. and Nicolet M. A., *Backscattering Spectroscopy* (Academic Press, New York) 1978.
[9] Feldman L. C. and Mayer J. W., *Fundamentals of Surface and Thin Film Analysis* (Elsevier Science Publishing Co.) 1986.
[10] Charity R. *et al.*, *Phys. Rev. C*, **82** (2010) 014610.
[11] Ono A. and Horiuchi H., *Prog. Part. Nucl. Phys.*, **53** (2004) 501.
[12] Lacroix *et al.*, *Phys. Rev. C*, **69** (2004) 054604.
[13] Brekiesz M. *et al.*, *Nucl. Phys. A*, **788** (2007) 224.
[14] Dell'Aquila D. *et al.*, *Nucl. Instrum. Methods A*, **877** (2018) 227.